

1

2

3

4 **Methods Optimization for the Expression and**
5 **Purification of Human Calcium Calmodulin-Dependent**
6 **Protein Kinase II Alpha**

7 **Scott C. Bolton^{1,2}, David H. Thompson², Tamara L. Kinzer-Ursem^{1*}**

8 ¹ Weldon School of Biomedical Engineering, Purdue University, West Lafayette, Indiana, United States of America

9 ² Department of Chemistry, Purdue University, West Lafayette, Indiana, United States of America

10 * Corresponding author

11 Email: tursem@purdue.edu (TKU)

12 **Abstract**

13 Calcium/calmodulin-dependent protein kinase II (CaMKII) is a complex multifunctional kinase that is highly
14 expressed in central nervous tissues and plays a key regulatory role in the calcium signaling pathway. Despite over 30 years of
15 recombinant expression and characterization studies, CaMKII continues to be investigated for its impact on signaling
16 cooperativity and its ability to bind multiple substrates through its multimeric hub domain. Here we compare and optimize
17 protocols for the generation of full-length wild-type human calcium/calmodulin-dependent protein kinase II alpha (CaMKII α).
18 Side-by-side comparison of expression and purification in both insect and bacterial systems shows that the insect expression
19 method provides superior yields of the desired autoinhibited CaMKII α holoenzymes. Utilizing baculovirus insect expression
20 system tools, our results demonstrate a high yield method to produce homogenous, monodisperse CaMKII in its autoinhibited
21 state suitable for biophysical analysis. Advantages and disadvantages of these two expression systems (baculovirus insect cell
22 versus *Escherichia coli* expression) are discussed, as well as purification optimizations to maximize the enrichment of full-
23 length CaMKII.

24 **Introduction**

25 The CaMKII protein family is composed of four similar genes identified as α , β , γ , and δ (1). While the isoforms γ ,
26 and δ are found ubiquitously in eukaryotic tissues, the α and β isoforms are found predominantly in the brain, making up 1-2%
27 of total protein in the hippocampus, and play a role in the regulation of synaptic plasticity in neurons (3). In the mammalian
28 brain CaMKII is found as a heterogeneous oligomer, or holoenzyme, of twelve or fourteen subunits assembled from a mix of
29 α and β isoforms (4–7). Each individual subunit includes a kinase domain incorporating a regulatory segment, an
30 oligomerization or hub domain, and a linker region joining the two domains whose length varies among isozymes. A number
31 of works have focused on the structural assembly of CaMKII and its mechanism of activation (1,6,7,11–15). It has been shown
32 that the close proximity of neighboring subunits within the holoenzyme enables rapid inter-subunit cross-phosphorylation
33 resulting in enzyme activation kinetics that are cooperative (13,16). Transmission electron microscopy, crystallography, and
34 small-angle x-ray scattering have been used to reveal the morphology of subunit assembly and estimate the range of movement
35 of the tethered kinase domains (6,7,11,12,17–20). To reduce the complexity of understanding these multi-subunit mechanisms,
36 these works have relied upon the recombinant expression of CaMKII where all subunits are of a single isozyme in the
37 autoinhibited state. For high resolution structural studies, highly-enriched, autoinhibited, monodisperse oligomeric CaMKII

38 enzyme is needed. Further, like many other kinases, CaMKII is labile and shows decreasing activity and aggregation over time
 39 (21,22). Thus, the conditions of purification and handling time must be optimized to ensure the recovery of the intact and
 40 functional CaMKII in high yield.

41 Many of the methods reported in the literature for generating purified recombinant CaMKII protein use bacterial
 42 expression or baculovirus insect expression, and these systems have employed non-tagged and polyhistidine tag fusion
 43 constructs. Table 1 lists the different purification strategies and yields (when given) that have been reported to date.

44 **Table 1. Purification Strategies for Recombinant Expression of Full-length CaMKII α .**

Reference	Expression	Mutations	Step 1 (pH)	Step 2 (pH)	Yield (mg/L)
Waxham (23)	<i>E. coli</i>	–	CS (7.5)	–	–
Brickey (25)	BEVS	–	AS (7.5)	CS	12 – 15
Hagiwara (24)	<i>E. coli</i>	–	AS (7.6)	CS (7.5)	–
Putkey (26)	BEVS	–	AS (7.5)	CS**	–
Kolb (27)	BEVS	–	CS (7.5)**	S	–
	BEVS	N-terminal 6xHis 1 – 382, 1 – 427	IMAC (7.5)	–	–
Kolodziej (6)	BEVS	–	AS	IMAC	–
Singla (28)	BEVS	–	PC (7.0)	CS (7.3)	–
Török (29)	BEVS	–	CS (7.5)	Q (7.5)	11
Rosenberg (12)	BEVS	D135N	S (7.4)	Q (8.3)*	0.005 – 0.01
Chao (13)	<i>E. coli</i>	C-terminal 6xHis	IMAC	Q (8.3)*	0.0025
Coultrap (30)	HEK293T	–	PC (7.0)	CS	–
Hoffman (10)	BEVS	–	CS (7.4)	–	–
Myers (20)	BEVS	–	PC (7.2)	CS	–

45 Legend: BEVS – baculovirus-insect expression vector system; AS – ammonium sulfate precipitation; CS –
 46 calmodulin-Sepharose affinity chromatography; S – cation exchange chromatography; Q – anion exchange chromatography;
 47 IMAC – Immobilized metal affinity chromatography; PC – phosphocellulose cation exchange chromatography; *followed by
 48 a gel filtration step; ** followed by a sucrose density centrifugation step.

49
 50 The Soderling lab first reported expression of recombinant wild type rat CaMKII α using a baculovirus-insect
 51 expression vector system (BEVS). It was explained that cell homogenization into lysate in the presence of glycine betaine, a
 52 zwitterionic osmolyte that aids in protein stabilization and solubilization, prevented CaMKII from forming aggregates that
 53 would precipitate from solution during centrifugation (25,31). The use of betaine in the lysis buffer resulted in improved
 54 recovery of CaMKII due to the added solubility, and this buffer is now commonly known as Brickey buffer. Using both
 55 ammonium sulfate precipitation and calmodulin-Sepharose (CaM-Sepharose) affinity chromatography purification steps, a
 56 final yield of 12 – 15 mg of purified CaMKII per liter of Sf9 cell culture was obtained, based an expression density of 3×10^6
 57 cells/mL. Török et al. reported a method omitting betaine, avoiding ammonium sulfate precipitation, and adding an anion

58 exchange chromatography step (29). Since betaine was not part of the protocol, the high yield might be due in part to the
59 presence of 10% fetal bovine serum (FBS) added to the Sf9 growth medium that has been shown to limit non-specific binding
60 of virus particles to cells and subsequently increase infection multiplicity (32).

61 The technique of Brickey et al. was adopted by the Waxham lab in a series of papers employing similar expression
62 conditions and lysis buffers but differed in their purification methods. Initially, the purification steps were combinations of
63 ammonium sulfate precipitation, CaM-Sepharose affinity chromatography, sucrose density gradient centrifugation, and
64 phosphocellulose cation exchange chromatography (1,6,26,27). These methods were eventually condensed to phosphocellulose
65 cation exchange chromatography followed by CaM-Sepharose affinity chromatography (20,28,30).

66 In the Kuriyan lab, Rosenberg et al. used similar expression conditions as Török et al. (without mention of FBS
67 supplementation) and modified the lysis buffer to replace betaine with 10% glycerol (12). Although purification described a
68 cation exchange chromatography step followed by an anion exchange chromatography step, an additional buffer exchange from
69 HEPES buffer (for cation exchange) to Tris buffer (for anion exchange) was likely required and may have contributed to loss
70 of CaMKII yield even before the final size-exclusion polishing step. Later, Chao et al. demonstrated the use of a bacterial
71 system to express CaMKII α (13). Bacterial kinases can phosphorylate heterologous human kinase, including CaMKII, and to
72 circumvent this problem the protein was co-expressed with λ -phosphatase (33). The CaMKII gene also fused a C-terminal
73 6xHis tag to facilitate crude separation from lysate by use of an Ni-NTA affinity chromatography step, which would ideally
74 capture full-length protein but not N-terminal truncated protein, though any C-terminal fragments due to full-length protein
75 cleavage would also be captured. The three-step purification process included immobilized metal affinity chromatography
76 (IMAC), anionic exchange chromatography and gel-filtration chromatography to produce 2.5 μ g of purified CaMKII per liter
77 of cells. Although this protocol has been used repeatedly, it requires large cultures (11,14,34–37).

78 Since the earliest reports of recombinant CaMKII expression over 30 years ago, studies of CaMKII continue to be
79 highly relevant for studying kinase structure and function and Ca²⁺-dependent cellular behavior (15,35–39). The process of
80 reconciling the many different purification methods using both expression systems motivated us to revisit the expression and
81 purification of CaMKII. Here we document an optimized method to minimize handling time while maximizing yield of this
82 labile enzyme.

83

84 **Materials and methods**

85 **Baculovirus Insect Expression of CaMKII.** A pFastBac vector (GenScript) incorporating the wild type human
86 CaMKII α isoform 2 gene at cloning site BamHI-XhoI was transformed into chemically competent DH10Bac cells and plated
87 on TKG (Tetracycline, Kanamycin and Gentamicin) plates. A single white colony was picked for bacmid prep and inoculated
88 into LB medium containing TKG and incubated at 37 °C with shaking at 225 rpm for 16 h. The cells were pelleted and the
89 baculovirus DNA extracted using a Qiagen mini-prep kit following the manufacturer's standard protocol. DNA was stored at
90 4 °C until use. ESF 921 growth medium (150 μ L, Expression Systems) without antibiotics was mixed with 9 μ L transfection
91 reactant in a 24 well plate before addition of 1 μ g baculovirus DNA and incubation at 20 °C for 30 min. Next, 850 μ L of Sf9
92 cells (2×10^6 cells/mL) were added to the well, sealed with a breathable membrane, and incubated for 5 h at 27 °C with 120 rpm
93 shaking. Media (3 mL) containing 10% heat inactivated FBS (Sigma F4135) was added and the cells were incubated at 27 °C
94 with 120 rpm shaking for 1 week. P0 viral stock was reserved from the supernatant of pellet centrifugation. Further viral
95 amplifications were performed using adherent Sf9 cells in a T-75 flask containing ESF 921 growth medium plus 5% heat-
96 inactivated FBS (Sigma) at 27 °C. After cells reached 50% confluence, 30 μ L of viral stock was added and allowed to incubate
97 4 – 5 days. The amplified virus preparation was harvested from the media by centrifugation at 300 x g for 10 min, then passed
98 through a sterile 0.22 μ m filter (VWR). Viral amplification was iterated four times, creating P1, P2, P3, and P4 preparations.
99 Lastly, protein expression was accomplished by incubating 2 mL of P4 stock (1:100 v/v) in a 1 L spinner flask (Corning)
100 containing 200 mL of Tni cells (Expression Systems LLC, Davis, CA) (1×10^6 cells/mL, unless otherwise stated) in ESF 921
101 growth medium at 27 °C with 140 rpm shaking. After 24 h, the culture was supplemented with 10 mL (5%) Boost Production
102 Additive (Expression Systems LLC, Davis, CA) where indicated. The culture was allowed to incubate with shaking for an
103 additional 48 h (unless otherwise indicated). Cells were pelleted at 300 x g for 10 min, washed once with buffer (50 mM
104 HEPES, pH 7.5, 200 mM NaCl, 1 mM EGTA and 1 mM EDTA) and pelleted again, then used immediately for purification or
105 flash frozen in liquid N₂ and stored at -80 °C.

106 **Bacterial Expression of CaMKII.** A pD444-SR cDNA vector (ATUM, Newark, CA) containing a T5 promoter, a
107 wild-type human CaMKII α isoform 1 gene codon-optimized for E. coli expression, and a λ -phosphatase gene was transformed
108 into chemically competent BL21-CodonPlus (DE3) (Agilent) cells following manufacture instructions and plated with
109 ampicillin. Successful colonies were picked and amplified in 5 mL of LB media containing ampicillin overnight at 37 °C with
110 shaking at 250 rpm. Protein was expressed by growing 200 μ L of culture overnight in 200 mL of LB containing ampicillin at

111 37 °C with shaking at 250 rpm until OD₆₀₀ = 0.8. Cell cultures were chilled to 4 °C, induced with 0.5 mM isopropyl β-D-1-
112 thiogalactopyranoside (IPTG) (Sigma) and 0.4 mM MnCl₂ and incubated at 16 °C with shaking at 250 rpm for 16 h (unless
113 otherwise indicated). Cells were harvested by centrifugation at 3000 x g at 4 °C for 15 min, washed once with buffer (50 mM
114 HEPES, pH 7.5, 200 mM NaCl, 1 mM EGTA and 1 mM EDTA), then flash frozen in liquid nitrogen and stored at -80 °C.

115 **Purification of CaMKII.** Insect cells were processed based on modifications to the method described by Singla et
116 al.(28) Briefly, frozen cells were thawed and re-suspended in ice-cold Brickey buffer (50 mM HEPES pH 7.2, 7.5 or 8.0, 5%
117 betaine, 1 mM EGTA, 1 mM EDTA, and 1X HALT protease inhibitor (Thermo Scientific)). Insect cells were homogenized on
118 ice with 10 strokes of a dounce homogenizer. Bacterial cells were incubated briefly with lysozyme on ice then lysed by probe
119 sonication. After homogenization, crude lysate from either insect or bacterial culture was clarified by centrifugation at 12,000
120 x g for 20 min at 4 °C, followed by ultracentrifugation of the supernatant at 100,000 x g for 1 h at 4 °C. The supernatant was
121 decanted and passed through a sterile 0.22 μm filter. The filtered sample was loaded at 0.5 mL/min onto an AKTA FPLC
122 system fitted with either a Mono S 5/50 GL column or freshly prepared 5 mL fine mesh cellulose phosphate column (Sigma
123 P/N C2258) equilibrated in binding buffer containing 50 mM HEPES (pH 7.2, 7.5 or 8.0), 100 mM NaCl, and 1 mM EGTA.
124 The column was washed with 5 column volumes (CV) of binding buffer, then eluted using a 100 mM – 1 M NaCl gradient in
125 4 CV. Peak fractions (typically 2 – 3 mL) were combined; 2 mM CaCl₂ and 10% glycerol were added and mixed. The sample
126 was then transferred to a 5 mL tube containing 300 μL CaM-Sepharose resin (GE Healthcare) equilibrated in 50 mM HEPES
127 (pH 7.2, 7.5 or 8.0), 2 mM CaCl₂, 200 mM NaCl, and 10% glycerol. The reaction mixture was incubated on a rotisserie for 1
128 h at 4 °C. The resin was washed 3 times (10 CV, followed by 6 CV, followed by another 6 CV) with wash buffer containing
129 50 mM HEPES (pH 7.5), 2 mM CaCl₂, 500 mM NaCl, and 10% glycerol. After each wash the resin was collected via
130 centrifugation at 500 x g for 5 min. The resin was then incubated twice for 15 min, each using 1 CV of elution buffer containing
131 50 mM HEPES (pH 7.5), 400 mM NaCl, 4 mM EGTA and 30% glycerol. Aliquots of eluted protein were immediately flash
132 frozen in liquid N₂ and stored at -80 °C. Protein concentration was measured by ultraviolet absorbance at 280 nm.

133 **Gel Electrophoresis and Western Blot.** All SDS-PAGE gel experiments were performed using 4% – 20% gradient
134 precast gels (BioRad Mini-PROTEAN) run at 170 V for 40 minutes in SDS Tris Glycine buffer. Dual Ladder, 2X Laemmli
135 buffer, equal volume loading. Blue Native PAGE gel experiments were performed in a cold room (4 °C) using 10% precast
136 gels (BioRad Mini-PROTEAN) and run at 170 V for 55 minutes. Coomassie gels were stained with GelCode Blue Safe Stain
137 (Thermo-Fisher, Waltham, MA) and imaged using a c600 gel imager (Azure Biosystems, Dublin, CA).

138 Western blots were performed using a semi-dry apparatus (BioRad) to transfer proteins from the precast SDS-PAGE
139 gel to a 0.45 μm polyvinylidene difluoride (PVDF) membrane. Transfers were run at 15 V for 30 minutes. Following transfer,
140 PVDF membranes were incubated with Pierce protein-free blocking buffer (Thermo-Fisher, Waltham, MA) for 30 minutes
141 under gentle rocking, followed by incubation with anti-CaMKII primary antibody 6G9 (Invitrogen MA1-048) diluted in buffer
142 (50% Tris-buffered saline buffer with 0.1% Tween-20 (TBS-T) + 50% blocking buffer) overnight. Membranes were then
143 washed 3X with TBS-T and incubated with secondary antibody (IRDye 680RD anti-mouse, Li-COR Biosciences GmbH) for
144 1 hour at room temperature with gentle rocking. Membranes were then washed 3X with TBS-T and imaged on a c600 gel
145 imager (Azure Biosystems, Dublin, CA).

146 **CaMKII Phosphorylation and Activity.** Phosphorylated CaMKII (Thr286P) was produced by a reaction previously
147 described by Bradshaw et al. (40) Briefly, a mixture containing 18 μM subunit CaMKII, 50 μM CaM, 500 μM ATP, 500 μM
148 CaCl_2 and 4 mM MgCl_2 was incubated on ice for 30 min. CaMKII phosphorylation was verified by Western blot staining with
149 22B1 anti-phospho-CaMKII antibody (Invitrogen MA1-047).

150 Kinase activity was determined by a radiolabeled ATP assay (21). A reaction mixture containing 50 mM HEPES, pH
151 7.5, 200 μM CaCl_2 , 10 mM MgCl_2 , 1 mg/mL BSA, 1 μM CaM, and 100 μM Syntide-2 was incubated at 30°C before adding
152 60 $\mu\text{Ci/mL}$ γ - ^{32}P ATP in 100 μM cold ATP. The reaction was started by the addition of 10 nM CaMKII α . Samples were spotted
153 onto Whatman P81 paper every 15 s for the first minute, then every 30 s for the next two minutes. Papers were washed with 75
154 mM phosphoric acid four times and allowed to dry before scintillation counting.

155 **Negative Stain TEM.** A final polishing step to confirm isolation of 12-mer CaMKII holoenzymes was performed
156 using a Superose 6 10/100 size-exclusion column resulting in an elution fraction of 20 $\mu\text{g/mL}$ in final buffer 20 mM HEPES,
157 pH 7.5, and 200 mM NaCl. The sample (3 μL) was then incubated on a glow-discharged, carbon-coated 400 mesh copper grid
158 (CF400-Cu, Electron Microscopy Sciences) for 1 min, followed by washing with three drops of a freshly-prepared 1% uranyl
159 formate solution, then wicked dry. Grids were imaged on an FEI Talos F200C equipped with a 4k x 4k BM-Ceta CCD camera
160 operating at 200 kV in low-dose mode (10 $\text{e}^-/\text{Å}^2\text{sec}$) at 73,000 X magnification and -5 μm defocus.

161 **Results**

162 **Expression of CaMKII**

163 CaMKII was expressed in both *E. coli* cells and Tni insect cells to compare and characterize the protein produced
164 from both systems. For both systems, lysis buffers incorporated betaine to improve protein solubility, resulting in the clarified
165 lysate containing the majority of the expressed CaMKII (25). For the bacterial expression method, BL21(DE3) cells were
166 transfected with two plasmids: one plasmid contained the CaMKII α isoform A gene (Q9UQM7-1) codon-optimized for *E. coli*
167 expression, and the second plasmid contained a Lambda-phosphatase gene used to dephosphorylate expressed CaMKII within
168 the cytoplasm. It is known that CaMKII expression in *E. coli* generates a significant fraction of truncation products, resulting
169 in a mixture of full-length subunits and kinase domain-truncated monomers (23,41). To mitigate this problem, expression was
170 carried out at a lower temperature of 16 °C. To observe the progression of CaMKII expression, 5 mL samples of expression
171 culture were collected at various timepoints post-induction, and the samples were lysed, clarified, and analyzed in a Western
172 blot stained with anti-CaMKII 6G9 that detects the kinase domain in both full-length and truncated subunits, and imaged with
173 a near infrared secondary antibody (Fig 1A). At all the time points tested, a band at 50 kD indicating expression of full length
174 CaMKII is seen, as is a second doublet band just below 37 kD that corresponds to the N-terminal truncated expression. All
175 bands appear to be maximal at 18 h, full-length CaMKII expression does not appear to increase beyond 18 h, and the doublet
176 band significantly decreases after 18 h. It was hypothesized that the doublet band below 37 kD may indicate the presence of a
177 phosphorylated truncation product. However, staining with an anti-phospho-CaMKII antibody 22B1 revealed no presence of
178 Thr286 phosphorylation (Fig 1B).

179

180 **Fig 1. Western blot analysis of CaMKII expression in clarified lysate as a function of time and expression system. (A)**

181 *E. coli* expression at various timepoints detected with primary antibody anti-CaMKII 6G9 followed by IRDye 680RD. (B) *E.*

182 *coli* expression (18 h) detected with primary antibody anti-phospho-CaMKII 22B1 followed by IRDye 680RD reveals no

183 presence of Thr286 phosphorylation. (C) Tni expression at various timepoints detected with primary antibody anti-CaMKII

184 6G9 followed by IRDye 680RD. (D) Tni expression (72 h) detected with primary antibody anti-phospho-CaMKII 22B1

185 followed by IRDye 680RD reveals no presence of Thr286 phosphorylation.

186

187 For CaMKII expression in BEVS, transfection and virus amplification was performed in adherent Sf9 cells, with

188 amplification culture media supplemented with 5% FBS to allow for improved adherence, higher multiplicity of infection

189 (MOI), and smaller volumes of intermediate titer stock. It was determined empirically that four iterations of 5-day amplification

190 were sufficient to produce a virus concentration suitable for protein expression. Expression of CaMKII was performed by
191 adding P4 virus to spinner cultures of Tni cells.

192 At various timepoints post-induction, samples of Tni cell culture were collected, lysed and clarified to perform
193 Western blots with anti-CaMKII 6G9 as was done with bacterial samples. In Fig 1C, lanes 48 h – 96 h show a band at 50 kD
194 expression of full-length CaMKII, a faint doublet band just above it, and a faint band at 30 kD. The bands appear strongest
195 after 72 h post-induction and continued up to 96 h post-induction. Similarly to *E. coli* expression, a Western blot stained with
196 a CaMKII phospho-antibody 22B1 showed that CaMKII was not phosphorylated at Thr286 (Fig 1D).

197 BEVS expression results shows a doublet band at 50 kD, which is not found in the bacterial expression data. This is
198 likely due to the small difference in sequences between the two expression systems. While the bacterial expression used
199 CaMKII α isoform Q9UQM7-1, BEVS expression used CaMKII α isoform Q9UQM7-2 which encodes a 12-mer nuclear
200 localization sequence (NLS) containing the residues KKRKSSSSVQLM. This addition is found at the end of the linker region
201 and has four consecutive serines that can be phosphorylated. Liquid chromatography – mass spectrometry (LC-MS-MS)
202 analysis on BEVS CaMKII confirmed that the protein was not phosphorylated at Thr286 (Table S1), Thr305 or Thr306 (Table
203 S2), but did show phosphorylation at the NLS serine residues in 53% of the fragment sequences (Table S3).

204 Three additional parameters for the baculovirus/insect expression vector system were evaluated to determine the effect
205 on protein yield: seed density, virus concentration, and the use of an expression additive to supplement the media (Fig 2). First,
206 to evaluate the effect of seeding density on protein expression, a side-by-side expression was conducted where one flask had a
207 starting cell count of 1×10^6 cells/mL and the other flask had a starting cell count of 2×10^6 cells/mL. Both flasks were infected
208 with 1% v/v P4 virus and incubated for 72 h. Samples (5 mL) of lysate from both flasks were lysed, clarified, and analyzed in
209 Western blots detected with primary antibody anti-CaMKII 6G9 followed by IRDye 680RD (Fig 2A). Both flasks appeared to
210 produce a similar amount of full-length CaMKII, yet the expression seeded with 2×10^6 cells/mL showed increased truncation
211 or degradation products.

212

213 **Fig 2. Analysis of baculovirus/insect expression parameters on the expression of CaMKII.** All figures are Western blots
214 stained with primary antibody anti-CaMKII 6G9 followed by IRDye 680RD. (A) Effect of seeding density of Tni cells before
215 infection. (B) Effect of virus concentration expressed as a percentage of P4 virus volume per volume of Tni culture. (C)
216 Effect of 5% BPA added 24 h post-infection (-BPA is no BPA added).

217

218 Next, the effect of virus concentration on the expression of CaMKII was evaluated. Three identical flasks were each
219 infected with 0.1%, 1% or 5% v/v virus. At 72 h post-infection, Western blots detected with primary antibody anti-CaMKII
220 6G9 followed by IRDye 680RD were performed on each culture (Fig 2B). The results demonstrate that the maximal expression
221 of full-length CaMKII at 50 kD occurred when the virus concentration was 0.1%, however this was also accompanied by
222 substantial bands of CaMKII truncation or degradation products, especially one prominent 30 kD band. Higher virus
223 concentrations of 1% and 5% showed less degradation, but also showed less full-length CaMKII formation, especially at 5%
224 virus concentration.

225 Boost Production Additive (BPA) (Expression Systems LLC, Davis, CA) is a nutrient boost for cells during late-stage
226 infection that may improve expression yield of some proteins. We examined the effect of using this additive on our expression
227 experiments. Two 72 h expression cultures were initiated with a seed density of 1×10^6 cells/mL and 1% v/v virus, with one
228 flask receiving 5% BPA after 24 h. Western blot stained with primary antibody anti-CaMKII 6G9 followed by IRDye 680RD
229 showed that BPA enabled a greater amount of full-length CaMKII and a slightly lighter band of truncated products (Fig 2C).

230 **Purification of CaMKII**

231 As discussed earlier and as shown in Table 1, many CaMKII purification protocols have used cation exchange
232 chromatography in their methods, though at different stages in the purification scheme and with different buffer pH values
233 (20,27,28,30,42). Our motivation to use ion exchange chromatography as the first step was twofold: to rapidly isolate full-
234 length CaMKII from lysate thus limiting potential protease activity, and to enrich CaMKII so that the subsequent calmodulin-
235 Sepharose resin incubation volume would be small. Additionally, a rapid elution gradient was chosen to minimize both the run
236 time and the elution volume. By fixing these parameters, we were able to evaluate electrostatic binding characteristics and
237 CaMKII enrichment across a range of buffer pH values.

238 Three purifications at varying pH of CaMKII from Tni clarified lysate at were performed side-by-side. The low range
239 of the pH value was bounded by both the ExPASy predicted isoelectric point of 6.6, and empirical data showing possible
240 aggregation of CaMKII under ischemic conditions at or below pH 6.8 (though this also requires activation by Ca^{2+} /CaM) (43–
241 46). Thus, we chose pH values sampling a range between pH 7.2 and pH 8.0. The results were analyzed by comparing Western
242 blot full-length CaMKII bands at 50 kD present in the elution fractions for each pH experiment (Fig 3A-3C) and (Fig S3).

243

244 **Fig 3. Effect of pH on CaMKII purification with cation-exchange chromatography.** Initial separation of CaMKII from
245 clarified lysate at (A) pH 7.2, (B) pH 7.5, and (C) pH 8.0. SDS-PAGE Western blot analysis detected with primary antibody
246 anti-CaMKII 6G9 followed by IRDye 680RD.

247

248 Purifications were made using frozen Tni cell pellets that were solubilized in Brickey buffer at the desired pH,
249 homogenized using a dounce homogenizer, clarified by ultracentrifugation, passed through a 0.22 μ m syringe filter, then
250 immediately loaded onto a Mono S column. In order to verify CaMKII binding to the column during loading, we took samples
251 during loading of the lysate onto the column (Fig 3A-3C, Flow through Peak lanes) and when the last of the flow through was
252 washed from the column (Fig 3A-3C, Flow through Tail lanes). A rapid elution gradient from 100 mM NaCl to 1 M NaCl was
253 used to elute CaMKII from the column (Fig 3A-3C, Elution 1-5 lanes).

254 The Western blot of CaMKII purified at pH 7.2 (Fig 3A) displayed a faint band at 50 kD in the flow through tail and
255 no bands in the elution fractions 1-5 which indicated that CaMKII did not bind the column. In contrast, Western blots of
256 purifications at pH 7.5 and pH 8.0 both demonstrate full-length CaMKII had bound to the column and was eluted from the
257 column (Fig 3B and 3C, Elution 1-5 lanes). At pH 7.5, CaMKII was eluted primarily in lanes 2 and 3, while at pH 8.0 CaMKII
258 was eluted in lanes 4 and 5, two column volumes later than pH 7.5. It should be noted that in all three blots in Fig 3, the clarified
259 lysate, flow through peak, and flow through tail lanes had highly diluted CaMKII which reduced the visibility of the bands,
260 while elution lanes 1-5 were enriched by a factor of 40 and had strongly visible bands. At pH 8.0 there were CaMKII
261 degradation products bound to the column that eluted in tandem with the full-length protein.

262 Phosphocellulose resin has found use as a cation exchange chromatography medium in CaMKII purification protocols
263 but has become increasingly difficult to purchase. The resin also requires extensive preparation including several rounds of
264 fines removal, careful washing in acidic pH and basic pH buffers, then equilibration in buffer before pouring the column. In
265 contrast, pre-packed ion-exchange columns are widely available and have robust handling characteristics including higher
266 pressure and solvents for regeneration. We evaluated the performance of these two cation exchange resins by performing a
267 side-by-side purification of CaMKII from clarified lysate with a 5 mL phosphocellulose column and a 1 mL Mono S column.
268 Although cation exchange purification rapidly performs an initial separation of CaMKII from a large volume of lysate, non-
269 specific protein debris in the eluted volume is still a significant problem. We employed a sequential CaM-Sepharose affinity

270 chromatography step using a small (300 μ L) fixed column volume in batch mode to further enrich CaMKII and remove cell
271 debris.

272 Additionally, this second purification step also acts to normalize CaMKII enrichment between the two cation exchange
273 chromatography columns (with differing elution volumes) and makes direct comparison a straightforward task. A schematic
274 describing the side-by-side comparison is shown in Fig 4. Briefly, a previously frozen 5 g Tni pellet (corresponding to 200 mL
275 of culture) containing expressed CaMKII was resuspended in Brickey lysis buffer, homogenized, clarified by
276 ultracentrifugation, then divided into two volumes of equal size. One volume was loaded onto a freshly prepared
277 phosphocellulose column and the other was loaded onto a Mono S column. Both columns used the same chromatography
278 buffers and elution gradient, resulting in a 25 mL elution volume for Mono S and 125 mL elution volume for phosphocellulose
279 (Fig 4). Each elution volume had 2 mM calcium and 10% glycerol added, followed by incubation with 300 μ L of CaM-
280 Sepharose resin on a rotisserie for one hour at 4 °C. After washing the resin, CaMKII was eluted with 4 mM EDTA. Since
281 CaM-Sepharose column volumes were identical, elution volumes were also identical thus normalizing the final concentrations.
282 The final CaMKII yield from the method incorporating Mono S was 4.0 mg/L of culture, nearly twice the final yield of 2.2
283 mg/L of culture from the method using phosphocellulose (Fig 5).

284

285 **Fig 4. Schematic detailing the comparison of the side-by-side two-step purification scheme.** The difference in column
286 volume sizes between Mono S and phosphocellulose are normalized by the CaM-Sepharose step, thereby making protein
287 concentration measurement between the two methods equivalent. Legend: CV – column volume.

288

289 **Fig 5. Side-by-side comparison of CaMKII initial separation by either phosphocellulose or Mono S cation exchange**
290 **chromatography, normalized by a second CaM-Sepharose affinity chromatography step.** SDS-PAGE followed by
291 Coomassie stain (A and C) or Western blots stained with 6G9 anti-CaMKII primary antibody and detected with
292 IRDye680RD secondary antibody (B and D). (A and B) use phosphocellulose for cation-exchange chromatography, and (C
293 and D) use Mono S for cation-exchange chromatography. Lanes were loaded with equal volumes. Lane representation: IN –
294 cation exchange chromatography combined elution fractions; FT – calmodulin-Sepharose flow through, WASH 1-3 – post-
295 incubation wash steps, ELUTION 1-2 – elution column volumes.

296

297 One unexpected artifact observed in Figs 3C and 3D is the band of CaMKII present in wash step 2 in the Mono S
298 purification that is not present in the phosphocellulose purification. This is attributed to some of the CaM-Sepharose resin
299 accidentally being washed away when decanting the wash buffer from the resin after centrifugation. While this is not a common
300 occurrence, we note that care must be taken when decanting after the wash and elution steps in batch reactions to maximize
301 protein recovery. A representative set of Mono S / CaM-Sepharose blots that do not have this artifact is shown in Fig S2.

302 **CaMKII yield comparison**

303 In the previous sections we screened the growth and expression conditions in bacterial and insect systems to produce
304 maximal full-length CaMKII in either system. We also optimized a two-stage purification system to enrich full-length CaMKII
305 from cell lysate. With these steps optimized, we compared the yields of bacterial and BEVS CaMKII produced by this same
306 two-stage chromatography method using bacterial and insect pellet masses of approximately 5 g each (Fig 6). Purification of
307 CaMKII from the bacterial expression system produced approximately 400 μg of full-length CaMKII per liter of culture at a
308 concentration of 0.45 mg/mL. This measurement, however, is compromised by the remaining impurity still found in the CaM-
309 Sepharose elution fractions, specifically two bands at approximately 100 kDa and 30 kDa that were bound and eluted from the
310 CaM-Sepharose resin (Fig 6A) but were not detected by anti-CaMKII antibody (Fig 6B). Purification of CaMKII from the
311 BEVS system produced approximately 4 mg of full-length CaMKII per liter of insect culture at a concentration of 0.5 mg/mL.

312

313 **Fig 6. Side-by-side CaMKII purification from bacteria and BEVS lysates.** The difference in column volume sizes
314 between Mono S and phosphocellulose are normalized by the CaM-Sepharose step, thereby making the protein concentration
315 measurement between the two methods equivalent. Legend: CV – column volume.

316

317 **Structural characterization**

318 The results shown in the SDS-PAGE gels in Figs 1-6 have demonstrated the production of monomeric full-length
319 CaMKII as desired. Next, we characterized the assembly of recombinant CaMKII into oligomers using three different methods.
320 First, a native polyacrylamide gel (7.5%) loaded with two-step purified CaMKII and stained with gel code blue showed a

321 primary diffuse band just above the 720 kDa marker (expected mass is 648 kDa) (Fig 7A). A second faint band can be seen
322 slightly higher which may represent the phosphorylation of the NLS. The second characterization method was to isolate
323 CaMKII species using a Superose 6 size-exclusion column. Elution produced a predominant peak of dodecameric CaMKII at
324 approximately 12 mL that coincides with a thyroglobulin standard peak at 660 kDa (Fig 7B) and also a minor flow through
325 peak of higher masses that are likely to be aggregates.

326

327 **Fig 7. Characterization of two-stage purified CaMKII obtained from BEVS** (A) Native PAGE followed by Coomassie
328 stain. (B) Superose 6 size-exclusion chromatogram. (C) Representative negative stain TEM micrograph of CaMKII oligomers.
329 Scale bar 20 nm.

330

331 Negative-stain TEM was used to characterize the morphology of CaMKII assembly into oligomers and confirm their
332 monodisperse distribution on the grid. The TEM micrographs collected showed the characteristic assembly of CaMKII: a hub-
333 and-spoke ring appearing in a face up orientation on the grid (Fig 7C). This morphology is consistent with prior observations
334 where a circular hub domain with a center pore is decorated by punctate kinase domains randomly distributed within several
335 nanometers of the hub circumference (6,7,11,20). It is important to note that protein adsorption to the TEM grid and the negative
336 staining procedure (blotting and sample dehydration) is expected to flatten and distort flexible oligomers such as CaMKII.

337 **Discussion and Conclusions**

338 Our motivation for this work is the exploration of the connected relationship between full-length protein expression
339 in high yield and a purification strategy that maximizes enrichment while limiting the handling time to minimize protein
340 degradation and aggregation.

341 Producing recombinant CaMKII in the lab remains a challenge. There are wide differences in the quality and quantity
342 of CaMKII produced from bacterial systems and baculovirus insect expression systems. There are also large differences in
343 purified protein yields obtained from the numerous purification schemes shown in the literature. Another consideration is the
344 lab environment and the equipment available to produce and purify the protein. These combined factors significantly affect the
345 yield of enriched, full-length dodecameric CaMKII available for experiments.

346 **Expression of CaMKII**

347 Bacterial expression systems are ubiquitous in laboratories and are easier to set up and maintain than BEVS, and the
348 cloning protocol is simpler than the multiple steps needed to produce baculovirus-infected insect cells. Bacterial cells
349 incorporating the CaMKII gene are easily stored as glycerol stocks and readily scaled up to express protein as needed. Despite
350 the ease of setup and use of bacterial systems, it is not always easier to produce full-length protein. Heterologous proteins may
351 contain rare codons that result in early termination of translation that produces unwanted truncated products. Undesired
352 phosphorylation of the target protein also requires effort to minimize. These difficulties may be ameliorated somewhat by the
353 careful selection of expression temperature, induction rate, the use of codon optimization in the gene sequence, and the co-
354 expression of phosphatases. Because the amount of full-length CaMKII produced per liter of bacterial culture is much less than
355 with BEVS culture, far more culture volume – and resulting lysate volume – must be processed which is not time and cost
356 efficient.

357 In contrast, insect cells require far more handling including regular passage, repeated growth and viability monitoring,
358 and days of infection with virus to produce the target protein or make additional virus. Eukaryotic insect cells are, however,
359 more friendly to mammalian kinases where codon usage is compatible, and genes may be cloned without codon substitutions.
360 Phosphorylation and other post-translational modifications are a concern for BEVS, and for CaMKII, we found the NLS serine
361 residues are phosphorylated during expression. Still, we found that the critical kinase-activation residues Thr286 and
362 Thr305/Thr306 are not phosphorylated and do not require a de-phosphorylation step to yield autoinhibited (inactive) CaMKII
363 when expressed in the BEVS system.

364 The first step compares protein expression quantity and contamination produced in clarified lysate between the best
365 protocols of each expression system. Our method for measuring CaMKII is by Western blot using the monoclonal antibody
366 6G9, which recognizes the N-terminal kinase domain of CaMKII. Since both full-length and partially translated protein will
367 contain some or all of the kinase domain, the 6G9 antibody is useful to detect even truncated protein species. We also use a
368 second phospho-specific antibody to detect the subpopulation of CaMKII that is phosphorylated at Thr286.

369 In the bacterial expression system, a qualitative comparison between full-length and truncated protein detected over
370 the expression time course shows that they are similar in amount in the first 24 hours, but the detection of these truncations
371 declines substantially over longer time periods (Fig 1A), likely due to proteasome activity or potentially sequestration and
372 excretion from the cells. Full-length CaMKII also appears to decrease after 18 hours, but not as markedly as the truncations.

373 Thus, a longer expression time improves the relative purity of full-length protein over truncated protein. However, if a
374 purification scheme can remove the truncations, then it is more beneficial to stop expression where full-length protein is
375 maximized. Our conclusion is that a lower expression temperature, gentle induction, and expression for 18 h yields a maximal
376 amount of full-length CaMKII provided that the large number of truncations can be removed efficiently.

377 In the BEVS, fewer truncations than full-length CaMKII are detected by Western blot, and these truncations do not
378 appear to degrade over time. Thus, it is helpful to optimize the initial conditions to limit truncations and increase yield. These
379 initial conditions include two interdependent factors: seeding density and infection concentration. The current study shows that
380 a 1% v/v infection concentration and culture at 1×10^6 cells/mL density allows for early-stage infection and cell doubling while
381 still providing enough nutrients to produce protein in late-stage infection (Fig 2A). Infection at a higher seed density (2×10^6
382 cells/mL) appears to increase degradation products without increasing full-length protein, likely because of the stress of cell
383 density and increased nutrient consumption. Interestingly, the increased degradation products are also seen when a culture of
384 1×10^6 cells/mL density is infected with 0.1% v/v virus concentration (Fig 2B). The low infection concentration allows for
385 more than one round of cell doubling and repeated virus amplification until late-stage infection is reached towards the end of
386 cell viability in the media. However, an initial virus concentration of 5% v/v produces a lower yield, because cell replication is
387 halted, and protein expression begins at or near the initial seeding density. Our conclusion is that seeding BEVS Tni cells at a
388 density of 1×10^6 cells/mL infected with 1% v/v produced a maximal ratio of full-length of CaMKII to truncations when
389 harvested at 72 h. Additionally, the use of BPA 24 h post-infection appears to produce an enhanced amount of full-length
390 protein expression with no relative increase in truncations (Fig 2C).

391 It is important to note that the doublet band found at 50 kD in the BEVS Western blots is likely due to our CaMKII
392 gene isoform B (Q9UQM7-2) that contains a short nuclear localization sequence (NLS). This addition inserts 12 residues
393 (KKRKSSSSVQLM) into the linker region that connects the kinase and hub domains. Proteomic analysis reveals that while
394 Thr286 and Thr305/Thr306 are not phosphorylated during expression in BEVS, the four NLS serine residues (Ser332 – Ser335)
395 are phosphorylated in 52% of the sample which can be seen as a distinct second band in SDS-PAGE. The phosphorylated
396 protein will have slightly lower mobility due to the increase in negative charge (47).

397 **CaMKII purification**

398 Having optimized full-length CaMKII expression in both systems, the next goal is to choose a purification strategy
399 that maximizes enrichment while limiting the handling time to minimize protein degradation. Some publications report the use

400 of CaMKII fused with polyhistidine tags to allow an IMAC crude separation from lysate, but this technique may present
401 obstacles. Bacterially expressed protein often includes fragments from proteolysis and expression truncation (41). If these
402 fragments also contain the fused histag, it will cause co-elution contamination that must be removed in subsequent steps. The
403 tags may be cleaved after expression, but this also requires further incubation time and purification steps which we wish to
404 avoid. Lastly, IMAC columns are not highly selective for the target protein and will bind many non-specific proteins. The
405 reduced flow rate needed to support the long residence time needed for histag binding, often 0.25 mL/min or less, translates to
406 nearly 3 h of processing time in our experiment. The eluted protein must still be enriched further, and imidazole must be
407 removed. Thus, we specifically chose to express and purify CaMKII without fusion tags.

408 Ammonium sulfate was used in the earliest publications and is very effective at protein enrichment of large volumes
409 of lysate, but it leaves many other proteases and contaminants in the resulting pellet. It also requires the removal of the
410 ammonium sulfate salt by another chromatographic step. Instead, the crude separation of clarified lysate using cation exchange
411 proves to be an effective method of isolating CaMKII quickly. Starting with 40 mL of clarified lysate and a loading rate of 1
412 mL/min onto the column, we can bind CaMKII to the column within 40 min and elute enriched protein with 5 column volumes
413 (5 mL) when using a Mono S column at pH 7.5. The smaller cation elution volume is advantageous when performing the next
414 enrichment step.

415 An interesting phenomenon is observed with cation exchange chromatography. Earlier publications report cationic
416 exchange purification buffers between pH 7–7.5. The theoretical isoelectric point for a full-length CaMKII subunit is
417 approximately 6.8, which should make it negatively charged above pH 7 and theoretically not bind cation resin. In our work,
418 we show that CaMKII very weakly binds cation resin at pH 7.2 (Fig 3A), which is congruent with a small net charge resulting
419 from a single, globular volume. As the pH increases, we would expect there to be no binding to the cation resin. Surprisingly,
420 the opposite occurs.

421 An explanation for this disparity may be that as the pH increases, the quaternary shape and exposed surfaces of
422 CaMKII may change. If we consider the catalytic and association domains of CaMKII independently, the kinase domain has a
423 theoretical pI of 8.05, and the association domain has a theoretical pI of 5.71. In order for CaMKII to bind strongly to the cation
424 resin at pH 8, the kinase domains may be in a state of extension away from the hub, revealing positively charged surfaces that
425 readily bind the cation resin. As seen in the results, a pH of 7.5 gave the best balance between good binding and efficient elution
426 into a minimal volume of buffer for subsequent steps (Fig 3B).

427 The comparison of the Coomassie stained gels and Western blot analyses of the freshly prepared phosphocellulose
428 column and the commercial Mono S column show similar amounts of full-length CaMKII and other non-specific debris.
429 Therefore, we conclude that the preparation time saved and long-term resin stability of Mono S make it a preferable choice for
430 the cation exchange chromatographic step.

431 Purification of CaMKII with CaM-Sepharose is widely used and can be done with either plug flow elution in EGTA
432 buffer (on an FPLC) or using a batch incubation method, as we perform here. Batch mode has two advantages for our
433 purification. First, we can use a much smaller volume of CaM-Sepharose resin slurry in a batch incubation than the typical 1
434 mL or 5 mL volume FPLC column. Thereby reducing the elution volume and increasing our enrichment. Second, it is also
435 straightforward to include glycerol, needed for cryo-preservation, in wash and elution buffers. With an FPLC, however, adding
436 glycerol to buffers increases the pressure against the column and often requires reducing and monitoring method flow rates to
437 run below the column pressure limit.

438 In side-by-side purifications of CaMKII from BEVS and bacterial expression using the Mono S / CaM-Sepharose
439 purification protocol, BEVS yielded ten-fold more full-length CaMKII per liter of culture than bacterial expression (an average
440 of 4 mg at 0.5 mg/mL versus 0.4 mg at 0.45 mg/mL, respectively).

441 In comparing our BEVS yield to earlier work, our method produced less protein than reported by Brickey et al.
442 Possible reasons for this discrepancy are reduced expression when using our viral construct in Tni cells, the loss of CaMKII in
443 the cation exchange chromatography flow through, and limiting the elution volume of that step to 5 column volumes in order
444 to minimize the CaM-Sepharose purification batch volume. Specific activity of our protein (5 $\mu\text{mol}/\text{min}/\text{mg}$) was consistent
445 with earlier reports and showed a linear response ($R^2=0.9989$) for at least 90 seconds (25,28) (Fig S5.) When we embarked on
446 the production of purified, recombinant CaMKII for our lab, the methods reported in the literature were diverse and the results
447 varied greatly. We hope that this detailed method optimization and comparison of methods provides clarity to the field for the
448 efficient and reproducible generation of full-length, recombinant CaMKII protein.

449 **Acknowledgments**

450 The authors thank Prof. Andy Hudmon (Department of Medicinal Chemistry and Molecular Pharmacology, Purdue
451 University) for his help in phosphocellulose preparation, and Dr. Keith Viccaro (Department of Medicinal Chemistry and
452 Molecular Pharmacology, Purdue University) for his help in collecting kinase activity data. We also thank the Purdue

453 Proteomics Facility for assistance with mass spectrometry data collection. We thank members of the Kinzer-Ursem lab for their
454 helpful comments on the manuscript.

455 **References**

- 456 1. Gaertner TR, Kolodziej SJ, Wang D, Kobayashi R, Koomen JM, Stoops JK, et al. Comparative analyses of the three-
457 dimensional structures and enzymatic properties of alpha, beta, gamma and delta isoforms of Ca²⁺-calmodulin-
458 dependent protein kinase II. *J Biol Chem*. 2004 Mar 26;279(13):12484–94.
- 459 2. Tombes RM, Faison MO, Turbeville JM. Organization and evolution of multifunctional Ca(2+)/CaM-dependent protein
460 kinase genes. *Gene*. 2003 Dec 11;322:17–31.
- 461 3. Erondu NE, Kennedy MB. Regional distribution of type II Ca²⁺/calmodulin-dependent protein kinase in rat brain. *J*
462 *Neurosci*. 1985 Dec;5(12):3270–7.
- 463 4. Bennett MK, Erondu NE, Kennedy MB. Purification and characterization of a calmodulin-dependent protein kinase that
464 is highly concentrated in brain. *J Biol Chem*. 1983 Oct 25;258(20):12735–44.
- 465 5. Woodgett JR, Davison MT, Cohen P. The calmodulin-dependent glycogen synthase kinase from rabbit skeletal muscle.
466 *European Journal of Biochemistry*. 1983;136(3):481–7.
- 467 6. Kolodziej SJ, Hudmon A, Waxham MN, Stoops JK. Three-dimensional reconstructions of calcium/calmodulin-
468 dependent (CaM) kinase IIalpha and truncated CaM kinase IIalpha reveal a unique organization for its structural core
469 and functional domains. *J Biol Chem*. 2000 May 12;275(19):14354–9.
- 470 7. Morris EP, Török K. Oligomeric structure of α -calmodulin-dependent protein kinase III Edited by A. R. Fersht. *Journal*
471 *of Molecular Biology*. 2001 Apr 20;308(1):1–8.
- 472 8. Okamoto KI, Narayanan R, Lee SH, Murata K, Hayashi Y. The role of CaMKII as an F-actin-bundling protein crucial
473 for maintenance of dendritic spine structure. *Proc Natl Acad Sci U S A*. 2007 Apr 10;104(15):6418–23.
- 474 9. Sanabria H, Swulius MT, Kolodziej SJ, Liu J, Waxham MN. β CaMKII regulates actin assembly and structure. *J*
475 *Biol Chem*. 2009 Apr 10;284(15):9770–80.
- 476 10. Hoffman L, Farley MM, Waxham MN. Calcium-calmodulin-dependent protein kinase II isoforms differentially impact
477 the dynamics and structure of the actin cytoskeleton. *Biochemistry*. 2013 Feb 19;52(7):1198–207.
- 478 11. Bhattacharyya M, Stratton MM, Going CC, McSpadden ED, Huang Y, Susa AC, et al. Molecular mechanism of
479 activation-triggered subunit exchange in Ca(2+)/calmodulin-dependent protein kinase II. *Elife*. 2016 Mar 7;5.
- 480 12. Rosenberg OS, Deindl S, Sung RJ, Nairn AC, Kuriyan J. Structure of the autoinhibited kinase domain of CaMKII and
481 SAXS analysis of the holoenzyme. *Cell*. 2005 Dec 2;123(5):849–60.
- 482 13. Chao LH, Pellicena P, Deindl S, Barclay LA, Schulman H, Kuriyan J. Intersubunit capture of regulatory segments is a
483 component of cooperative CaMKII activation. *Nat Struct Mol Biol*. 2010 Mar;17(3):264–72.
- 484 14. Stratton M, Lee IH, Bhattacharyya M, Christensen SM, Chao LH, Schulman H, et al. Activation-triggered subunit
485 exchange between CaMKII holoenzymes facilitates the spread of kinase activity. *Elife*. 2014 Jan 28;3:e01610.
- 486 15. Karandur D, Bhattacharyya M, Xia Z, Lee YK, Muratcioglu S, McAfee D, et al. Breakage of the oligomeric CaMKII
487 hub by the regulatory segment of the kinase. *Elife*. 2020 Sep 9;9.

- 488 16. Johnson DE, Hudmon A. Activation State-Dependent Substrate Gating in Ca(2+)/Calmodulin-Dependent Protein Kinase
489 II. *Neural Plast.* 2017;2017:9601046.
- 490 17. Hoelz A, Nairn AC, Kuriyan J. Crystal structure of a tetradecameric assembly of the association domain of
491 Ca²⁺/calmodulin-dependent kinase II. *Mol Cell.* 2003 May;11(5):1241–51.
- 492 18. Rellos P, Pike AC, Niesen FH, Salah E, Lee WH, von Delft F, et al. Structure of the CaMKII δ /calmodulin complex
493 reveals the molecular mechanism of CaMKII kinase activation. *PLoS Biol.* 2010 Jul 27;8(7):e1000426.
- 494 19. Chao LH, Stratton MM, Lee IH, Rosenberg OS, Levitz J, Mandell DJ, et al. A mechanism for tunable autoinhibition in
495 the structure of a human Ca²⁺/calmodulin-dependent kinase II holoenzyme. *Cell.* 2011 Sep 2;146(5):732–45.
- 496 20. Myers JB, Zaegel V, Coultrap SJ, Miller AP, Bayer KU, Reichow SL. The CaMKII holoenzyme structure in activation-
497 competent conformations. *Nat Commun.* 2017 Jun 7;8:15742.
- 498 21. Hudmon A, Aronowski J, Kolb SJ, Waxham MN. Inactivation and self-association of Ca²⁺/calmodulin-dependent
499 protein kinase II during autophosphorylation. *J Biol Chem.* 1996 Apr 12;271(15):8800–8.
- 500 22. Hudmon A, Kim SA, Kolb SJ, Stoops JK, Waxham MN. Light scattering and transmission electron microscopy studies
501 reveal a mechanism for calcium/calmodulin-dependent protein kinase II self-association. *J Neurochem.* 2001
502 Mar;76(5):1364–75.
- 503 23. Waxham MN, Aronowski J, Kelly PT. Functional analysis of Ca²⁺/calmodulin-dependent protein kinase II expressed in
504 bacteria. *J Biol Chem.* 1989 May 5;264(13):7477–82.
- 505 24. Hagiwara T, Ohsako S, Yamauchi T. Studies on the regulatory domain of Ca²⁺/calmodulin-dependent protein kinase II
506 by expression of mutated cDNAs in *Escherichia coli*. *J Biol Chem.* 1991 Sep 5;266(25):16401–8.
- 507 25. Brickey DA, Colbran RJ, Fong YL, Soderling TR. Expression and characterization of the alpha-subunit of
508 Ca²⁺/calmodulin-dependent protein kinase II using the baculovirus expression system. *Biochem Biophys Res Commun.*
509 1990 Dec 14;173(2):578–84.
- 510 26. Putkey JA, Waxham MN. A peptide model for calmodulin trapping by calcium/calmodulin-dependent protein kinase II.
511 *J Biol Chem.* 1996 Nov 22;271(47):29619–23.
- 512 27. Kolb SJ, Hudmon A, Ginsberg TR, Waxham MN. Identification of domains essential for the assembly of
513 calcium/calmodulin-dependent protein kinase II holoenzymes. *J Biol Chem.* 1998 Nov 20;273(47):31555–64.
- 514 28. Singla SI, Hudmon A, Goldberg JM, Smith JL, Schulman H. Molecular characterization of calmodulin trapping by
515 calcium/calmodulin-dependent protein kinase II. *J Biol Chem.* 2001 Aug 3;276(31):29353–60.
- 516 29. Torok K, Tzortzopoulos A, Grabarek Z, Best SL, Thorogate R. Dual effect of ATP in the activation mechanism of brain
517 Ca(2+)/calmodulin-dependent protein kinase II by Ca(2+)/calmodulin. *Biochemistry.* 2001 Dec 11;40(49):14878–90.
- 518 30. Coultrap SJ, Bayer KU. Ca²⁺/Calmodulin-Dependent Protein Kinase II (CaMKII). In: Mukai H, editor. *Protein Kinase*
519 *Technologies*. Totowa, NJ: Humana Press; 2012. p. 49–72.
- 520 31. Leibly DJ, Nguyen TN, Kao LT, Hewitt SN, Barrett LK, Van Voorhis WC. Stabilizing additives added during cell lysis
521 aid in the solubilization of recombinant proteins. *PLoS One.* 2012;7(12):e52482.
- 522 32. Maranga L, Coroadinha AS, Carrondo MJ. Insect cell culture medium supplementation with fetal bovine serum and
523 bovine serum albumin: effects on baculovirus adsorption and infection kinetics. *Biotechnol Prog.* 2002 Aug;18(4):855–
524 61.

- 525 33. Shrestha A, Hamilton G, O'Neill E, Knapp S, Elkins JM. Analysis of conditions affecting auto-phosphorylation of
526 human kinases during expression in bacteria. *Protein Expr Purif.* 2012 Jan;81(1):136–43.
- 527 34. McSpadden ED, Xia Z, Chi CC, Susa AC, Shah NH, Gee CL, et al. Variation in assembly stoichiometry in non-
528 metazoan homologs of the hub domain of Ca(2+)/calmodulin-dependent protein kinase II. *Protein Sci.* 2019
529 Jun;28(6):1071–82.
- 530 35. Sloutsky R, Dziedzic N, Dunn MJ, Bates RM, Torres-Ocampo AP, Boopathy S, et al. Heterogeneity in human
531 hippocampal CaMKII transcripts reveals allosteric hub-dependent regulation. *Sci Signal.* 2020 Jul 21;13(641).
- 532 36. Torres-Ocampo AP, Ozden C, Hommer A, Gardella A, Lapinskas E, Samkutty A, et al. Characterization of
533 CaMKIIalpha holoenzyme stability. *Protein Sci.* 2020 Jun;29(6):1524–34.
- 534 37. Ozden C, Sloutsky R, Mitsugi T, Santos N, Agnello E, Gaubitz C, et al. CaMKII binds both substrates and activators at
535 the active site. *Cell Rep.* 2022 Jul 12;40(2):111064.
- 536 38. Hoffman L, Li L, Alexov E, Sanabria H, Waxham MN. Cytoskeletal-like Filaments of Ca(2+)-Calmodulin-Dependent
537 Protein Kinase II Are Formed in a Regulated and Zn(2+)-Dependent Manner. *Biochemistry.* 2017 Apr 18;56(15):2149–
538 60.
- 539 39. Bhattacharyya M, Lee YK, Muratcioglu S, Qiu B, Nyayapati P, Schulman H, et al. Flexible linkers in CaMKII control
540 the balance between activating and inhibitory autophosphorylation. *Elife.* 2020 Mar 9;9.
- 541 40. Bradshaw JM, Kubota Y, Meyer T, Schulman H. An ultrasensitive Ca²⁺/calmodulin-dependent protein kinase II-protein
542 phosphatase 1 switch facilitates specificity in postsynaptic calcium signaling. *Proc Natl Acad Sci U S A.* 2003 Sep
543 2;100(18):10512–7.
- 544 41. Praseeda M, Beena MK, Asha SJ, Omkumar RV. The C-terminus of CaMKII is truncated when expressed in *E. coli*.
545 *Protein Pept Lett.* 2004 Apr;11(2):175–9.
- 546 42. Rosenberg OS, Deindl S, Sung RJ, Nairn AC, Kuriyan J. Structure of the Autoinhibited Kinase Domain of CaMKII and
547 SAXS Analysis of the Holoenzyme. *Cell.* 2005 Dec 2;123(5):849–60.
- 548 43. Dosemeci A, Reese TS, Petersen J, Tao-Cheng JH. A novel particulate form of Ca(2+)/calmodulin-dependent
549 [correction of Ca(2+)/CaMKII-dependent] protein kinase II in neurons. *J Neurosci.* 2000 May 1;20(9):3076–84.
- 550 44. Hudmon A, Lebel E, Roy H, Sik A, Schulman H, Waxham MN, et al. A mechanism for Ca²⁺/calmodulin-dependent
551 protein kinase II clustering at synaptic and nonsynaptic sites based on self-association. *J Neurosci.* 2005 Jul
552 27;25(30):6971–83.
- 553 45. Vest RS, O'Leary H, Bayer KU. Differential regulation by ATP versus ADP further links CaMKII aggregation to
554 ischemic conditions. *FEBS Lett.* 2009 Nov 19;583(22):3577–81.
- 555 46. Wilkins MR, Gasteiger E, Bairoch A, Sanchez JC, Williams KL, Appel RD, et al. Protein identification and analysis
556 tools in the ExPASy server. *Methods Mol Biol.* 1999;112:531–52.
- 557 47. Lee CR, Park YH, Min H, Kim YR, Seok YJ. Determination of protein phosphorylation by polyacrylamide gel
558 electrophoresis. *J Microbiol.* 2019 Feb;57(2):93–100.

559 **Supporting information**

560

561 **S1 Fig. Mono S chromatograms of CaMKII crude separation at three different working pH values.** (A) pH 7.2, (B) pH
562 7.5, (C) pH 8.0.

563

564 **S2 Fig. Representative SDS-PAGE Coomassie gel and 6G9 Western blot of the two-step Mono S / CaM-Sepharose**
565 **purification.** (A). SDS-PAGE followed by Coomassie stain, (B) Western blots stained with 6G9 anti-CaMKII primary
566 antibody and detected with IRDye680RD secondary antibody.

567

568 **S3 Fig. Effect of pH on CaMKII purification with cation-exchange chromatography.** Initial separation of CaMKII from
569 clarified lysate at (A) pH 7.2, (B) pH 7.5, and (C) pH 8.0. SDS-PAGE followed by Coomassie stain directly corresponds to the
570 Western blots in Fig 3.

571

572 **S4 Fig. CaMKII specific activity after purification.** Radiolabeled ATP assay shows a linear response for at least 90 seconds.
573 Specific activity is 5 $\mu\text{mol}/\text{min}/\text{mg}$. Error bars represent $n=3$.

574

575 **S1 Table. Liquid chromatography mass spectrometry detection of CaMKII α isoform B phosphorylation at Thr 286.**

Fragment Sequence	Number of Sites	
	Phosphorylated	
	0	1
HPWISHRSTVASC MHRQETVDCLK	9	0
QETVDCLK	9	0
QETVDCLKK	11	0
QETVDCLKK	0	1
QETVDCLKKFNAR	5	0

STVASCMLHRQETVDCLKK	1	0
Total Unmodified Counts	35	
Total Phosphorylated Counts	1	
Fraction Phosphorylated (%)	3	

576

577 **S2 Table. Liquid chromatography mass spectrometry detection of CaMKII α isoform B phosphorylation at Thr 305 /**
 578 **Thr 306.**

Fragment Sequence	Number of Sites Phosphorylated		
	0	1	2
GAILTTMLATR	98	0	0
GAILTTMLATR	0	2	0
GAILTTMLATRNFSGGK	1	0	0
KLKGAILTTMLATR	2	0	0
LKGAILTTMLATR	34	0	0
LKGAILTTMLATRNFSGGK	1	0	0
Total Unmodified Counts	136		
Total Phosphorylated Counts	2		
Fraction Phosphorylated (%)	1		

579

580 **S3 Table. Liquid chromatography mass spectrometry detection of CaMKII α isoform B phosphorylation at the nuclear**
 581 **localization sequence (Ser 332/333/334/335).**

Fragment Sequence	Number of Sites Phosphorylated

	0	1	2	3	4	5
KSSSSVQLMESSESTNTTIEDEDTK	82	82	19	10	7	0
KSSSSVQLMESSESTNTTIEDEDTKVR	5	9	5	13	9	7
RKSSSSVQLMESSESTNTTIEDEDTK	0	16	14	6	5	0
SSSSVQLMESSESTNTTIEDEDTK	127	43	4	10	4	0
SSSSVQLMESSESTNTTIEDEDTKVR	57	15	3	15	11	0
Subtotal	271	165	45	54	36	7
Total Unmodified Counts	271					
Total Phosphorylated Counts	307					
Fraction Phosphorylated (%)	53					

582

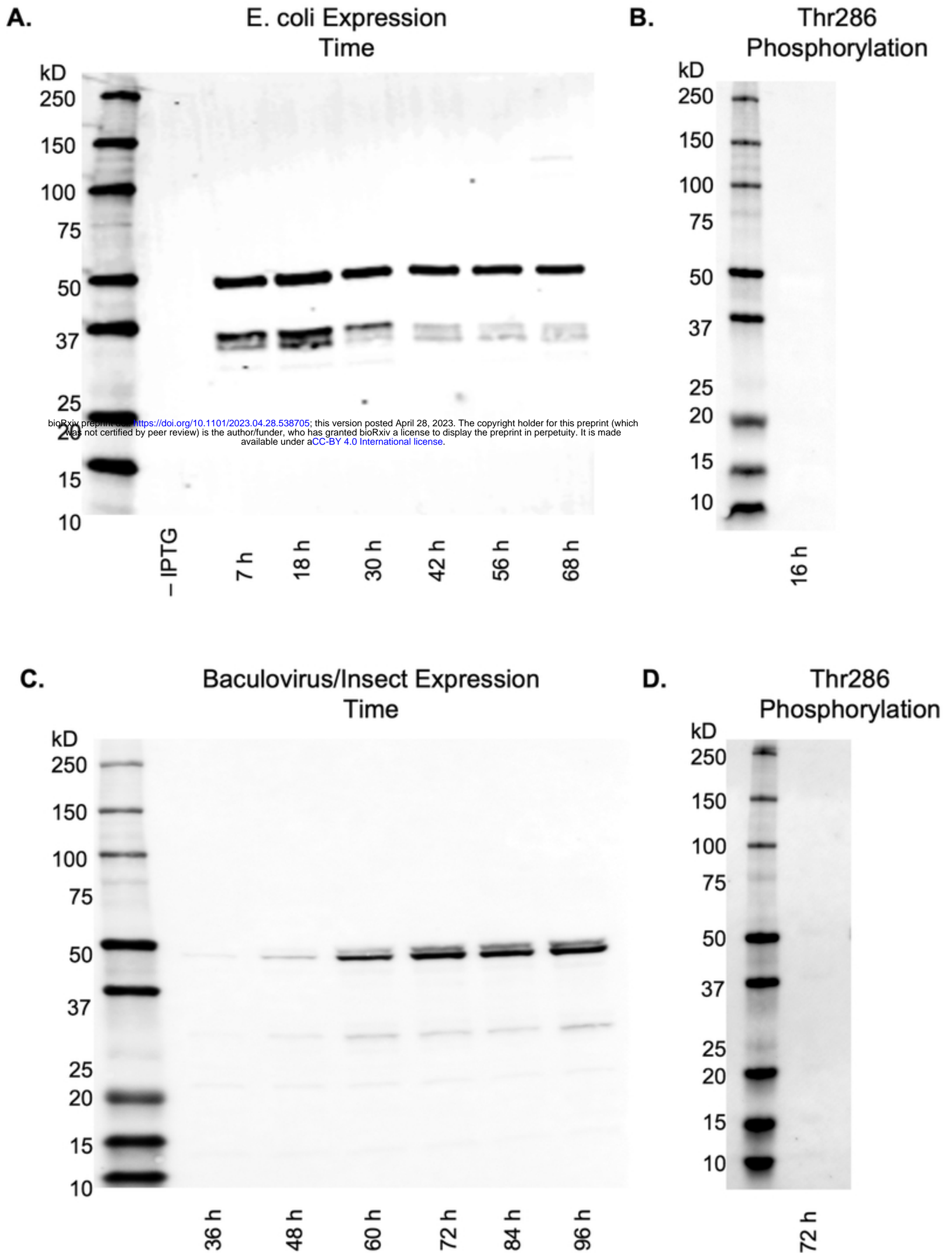


Figure 1

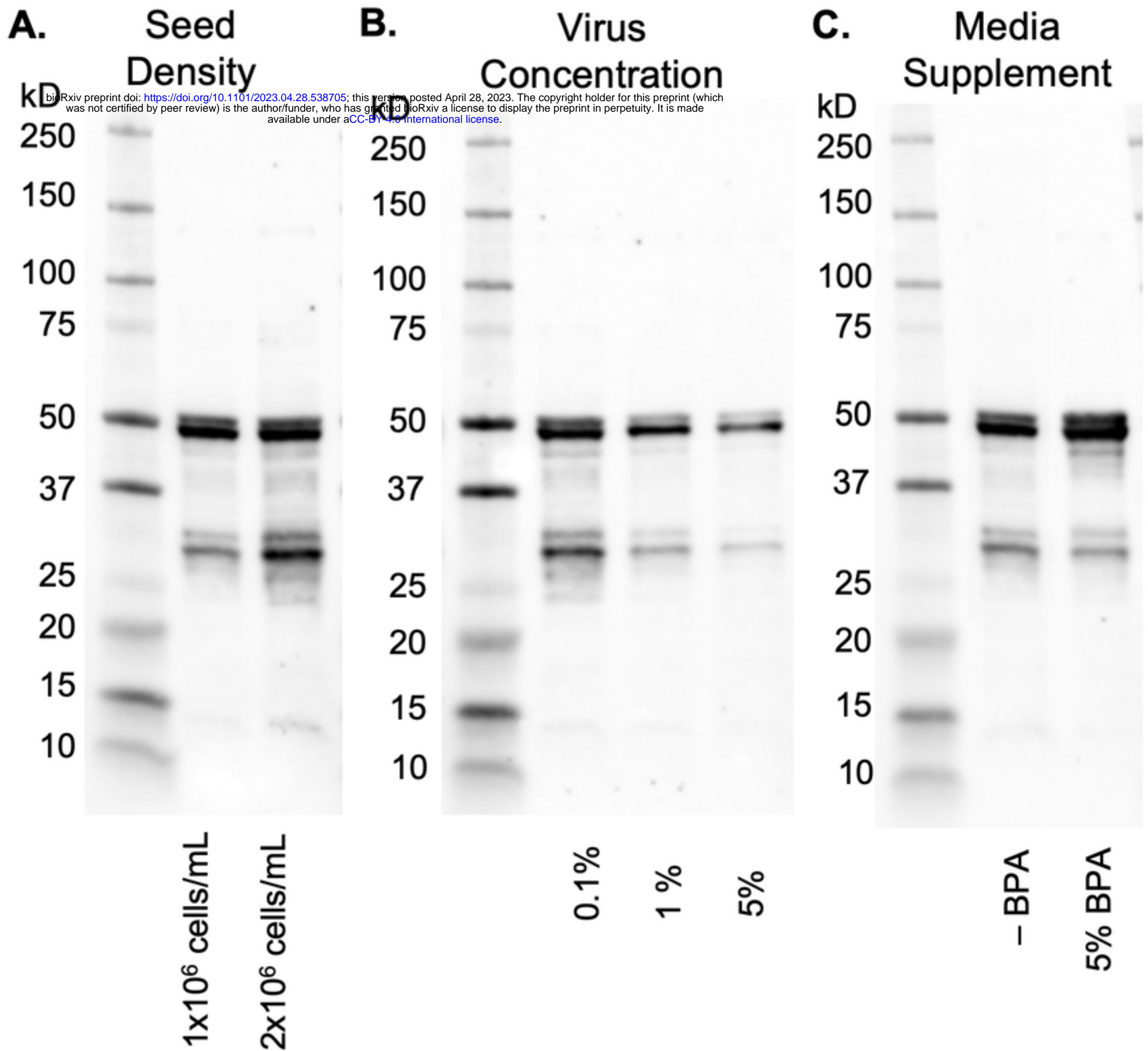


Figure 2

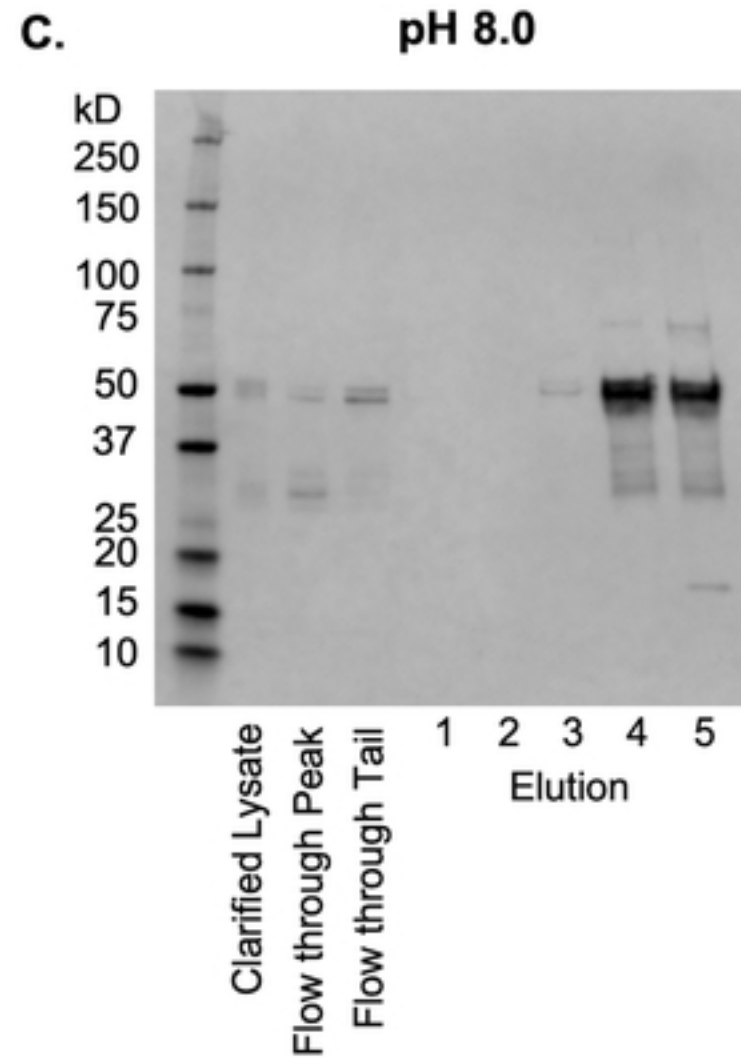
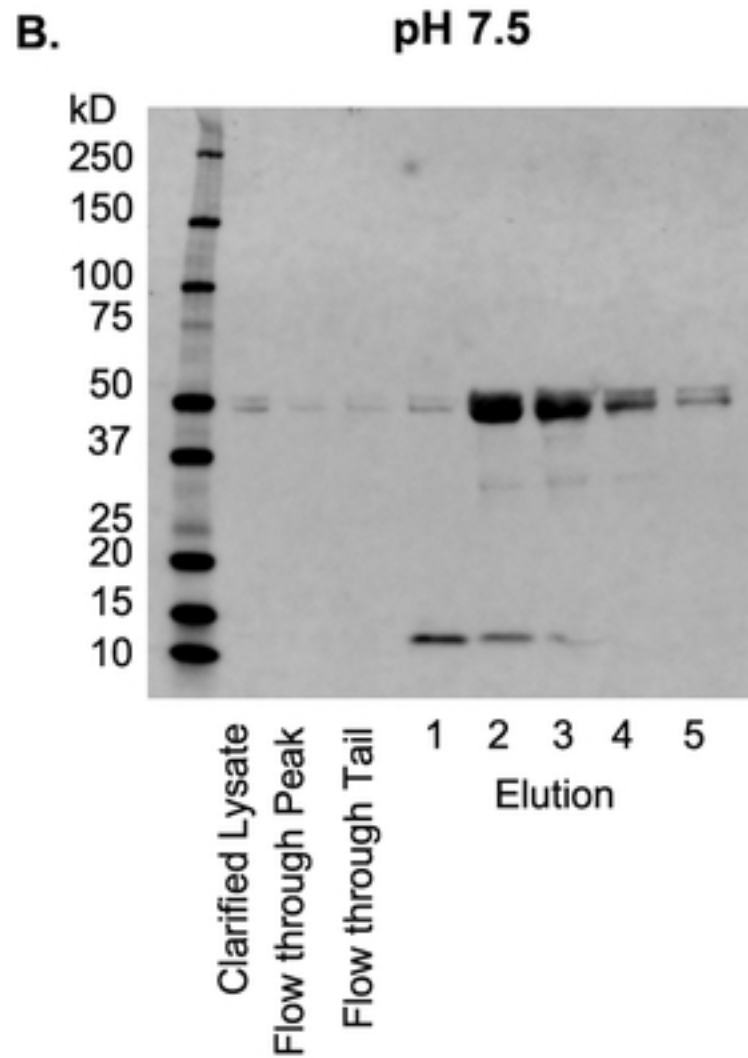
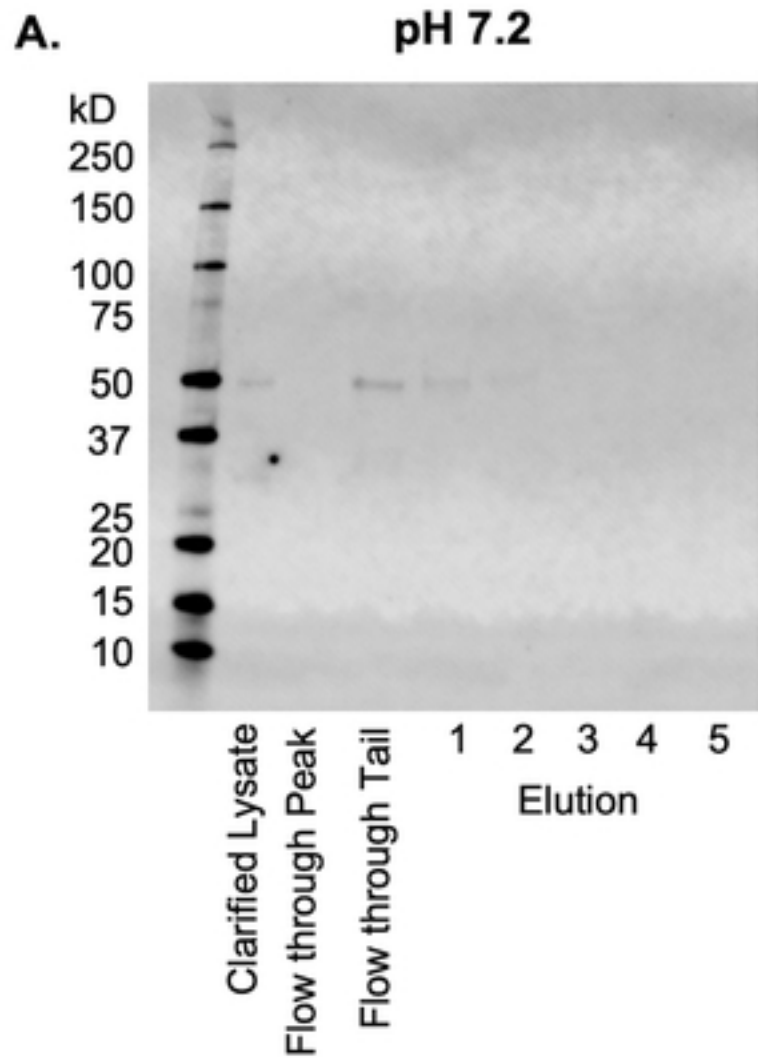


Figure 3

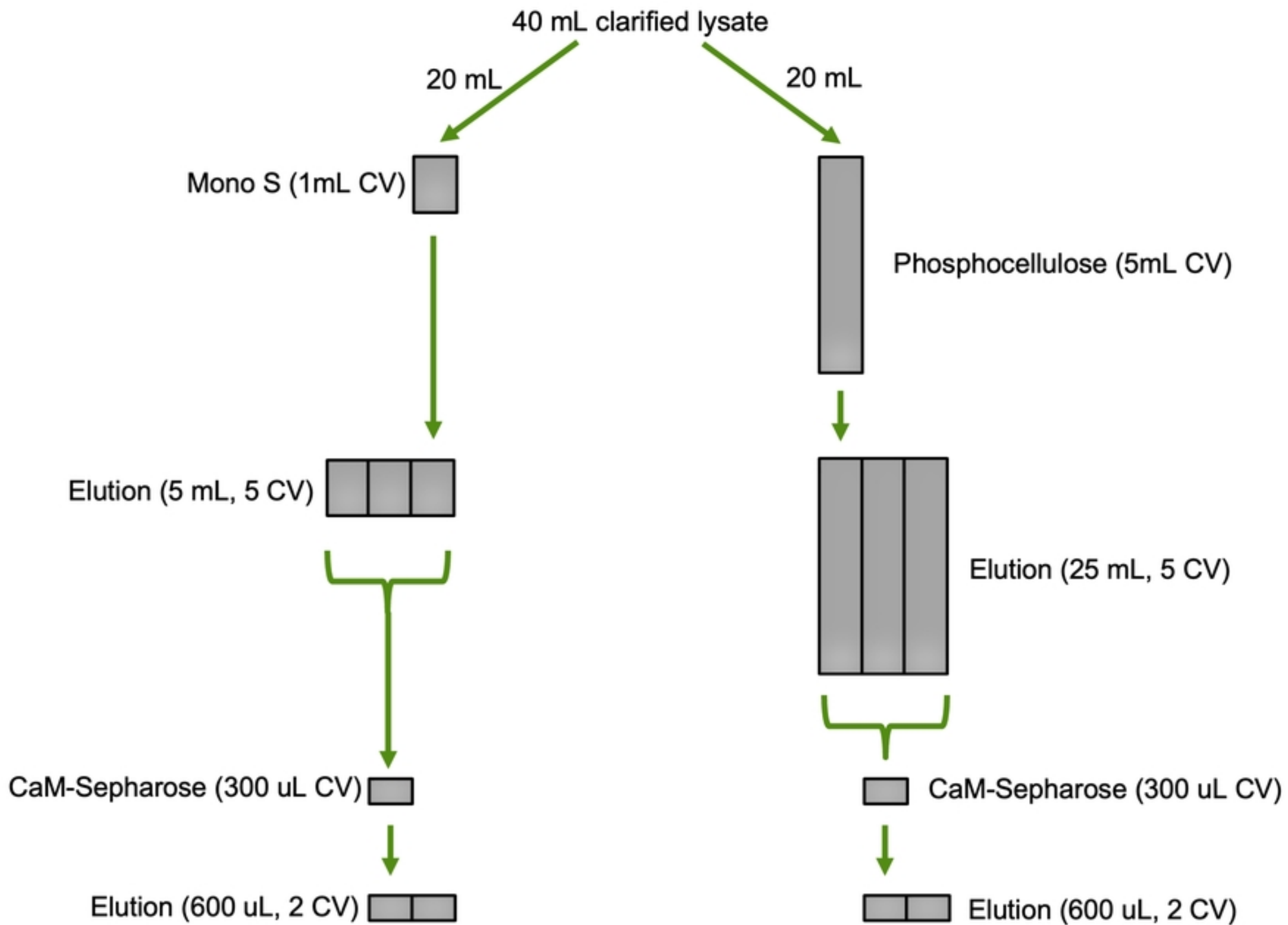
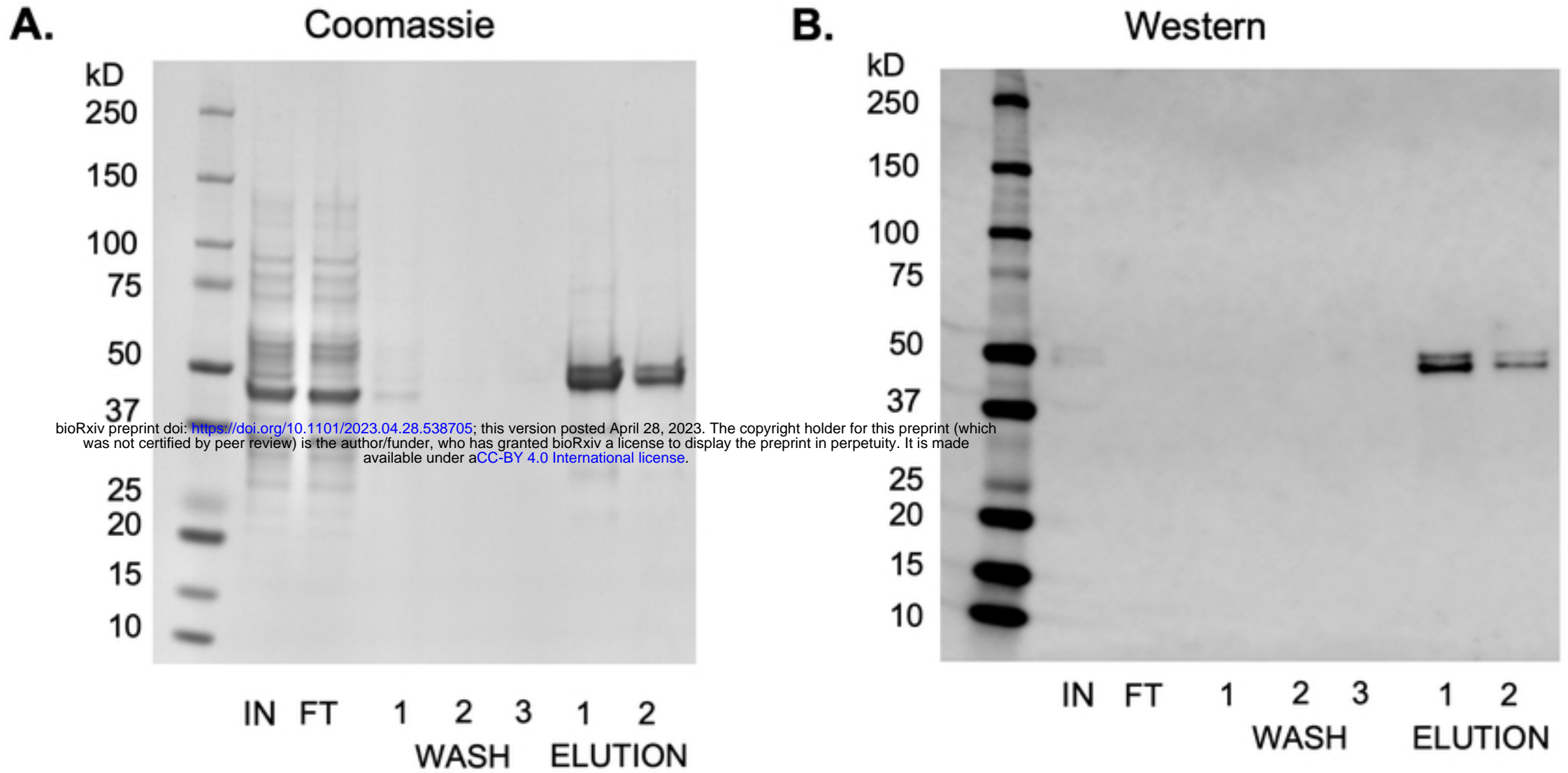


Figure 4

Phosphocellulose followed by CaM-Sepharose



Mono S followed by CaM-Sepharose

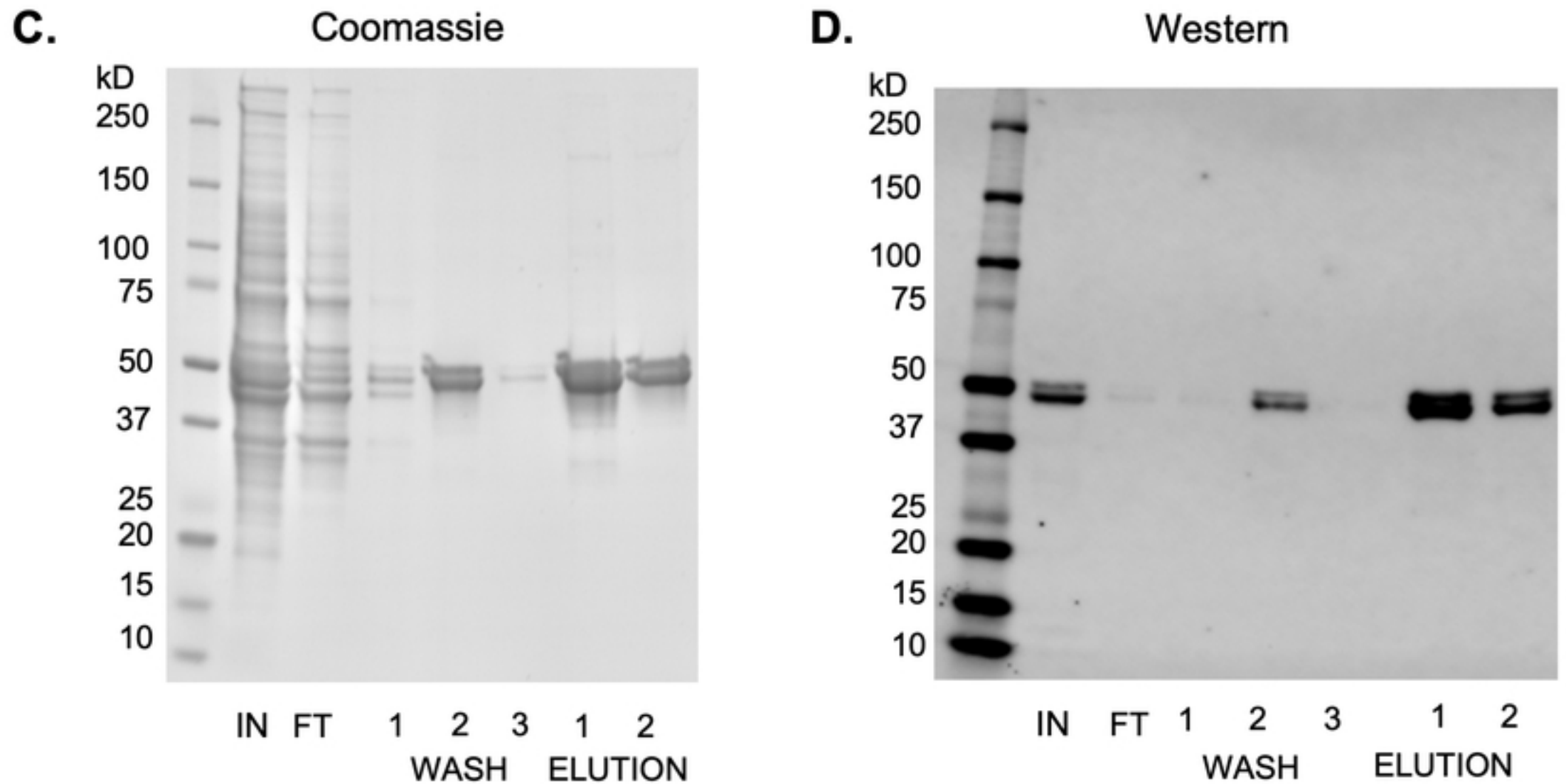
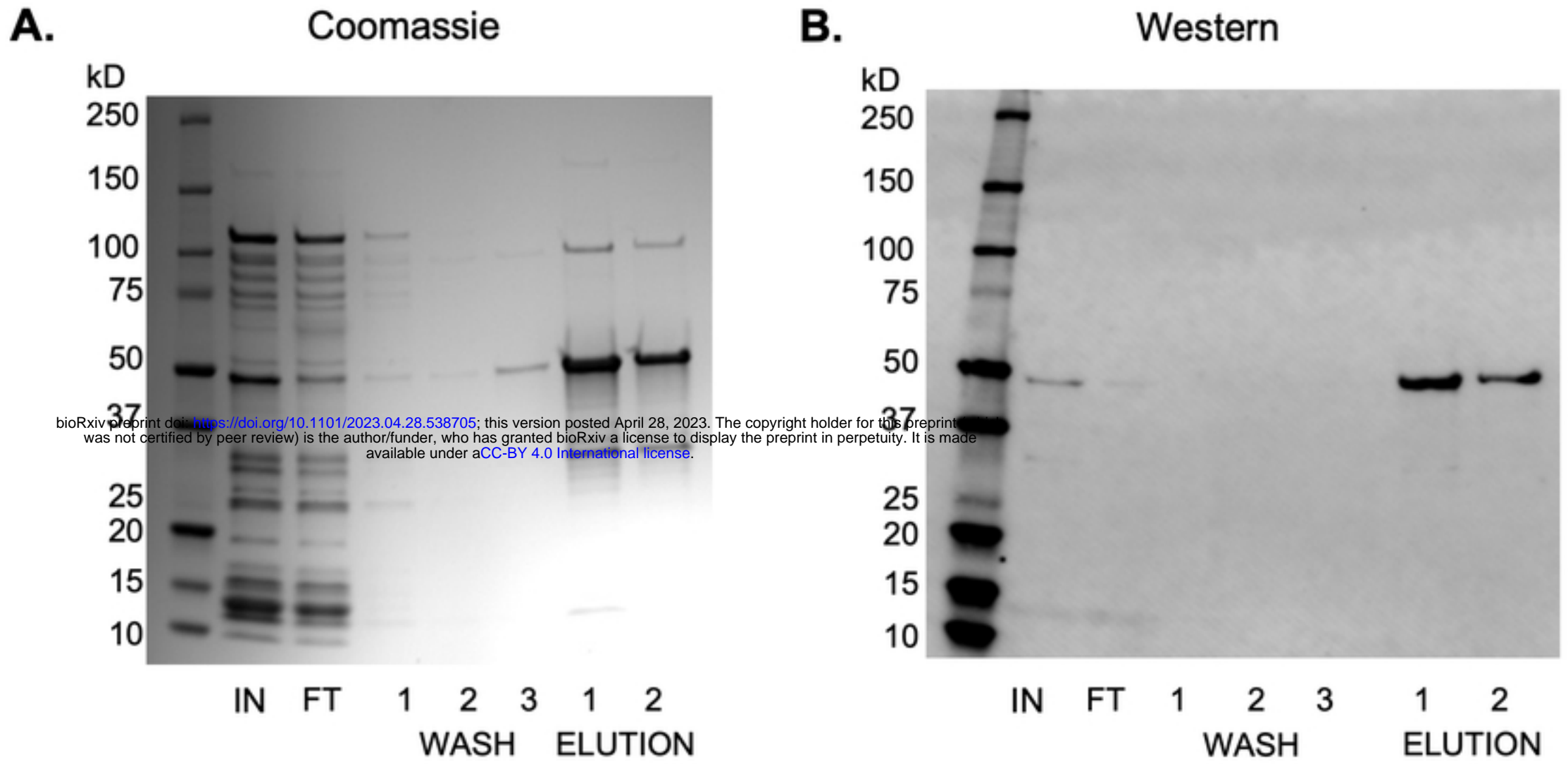


Figure 5

Bacterial Expression



BEVS Expression

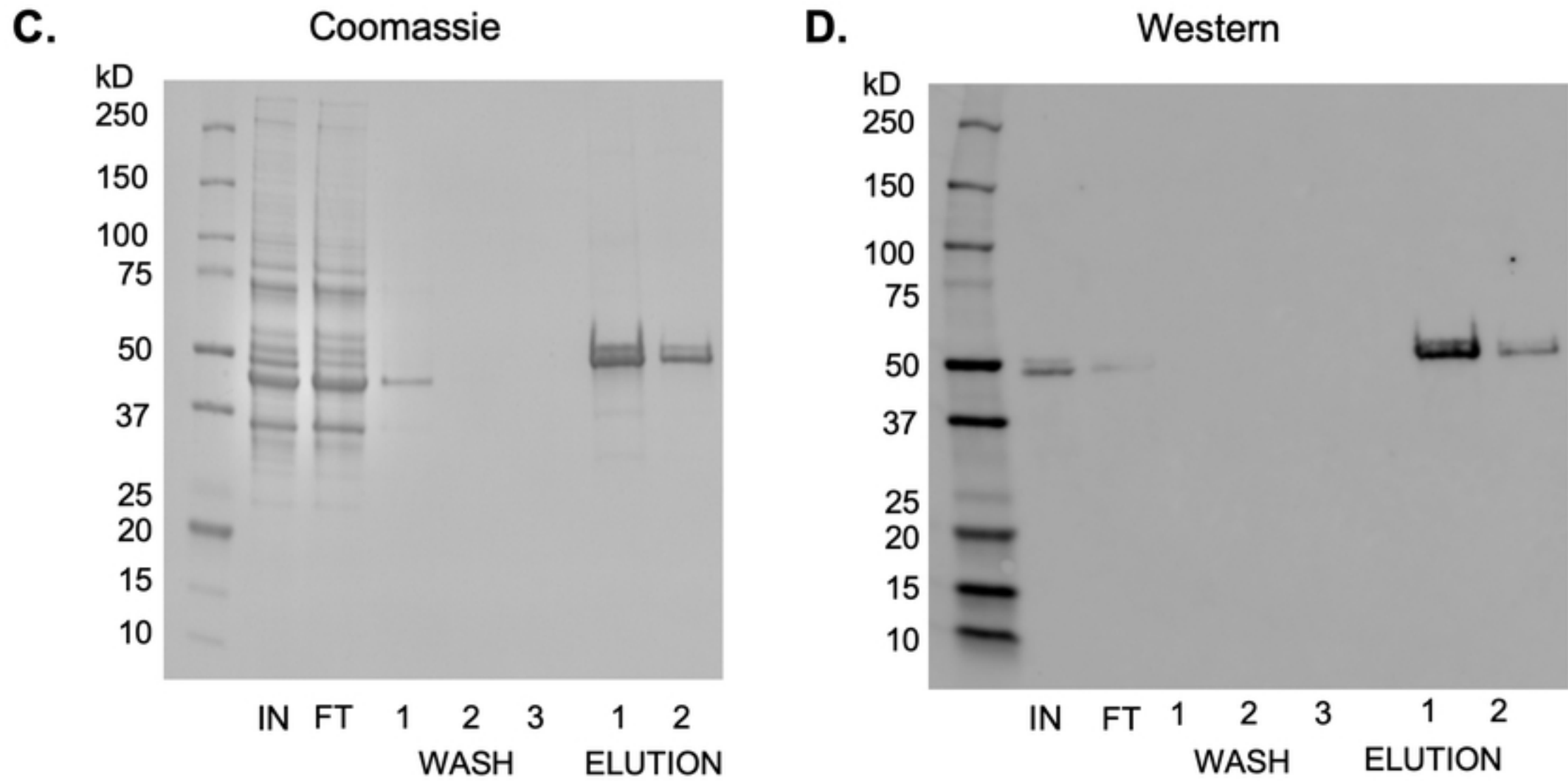
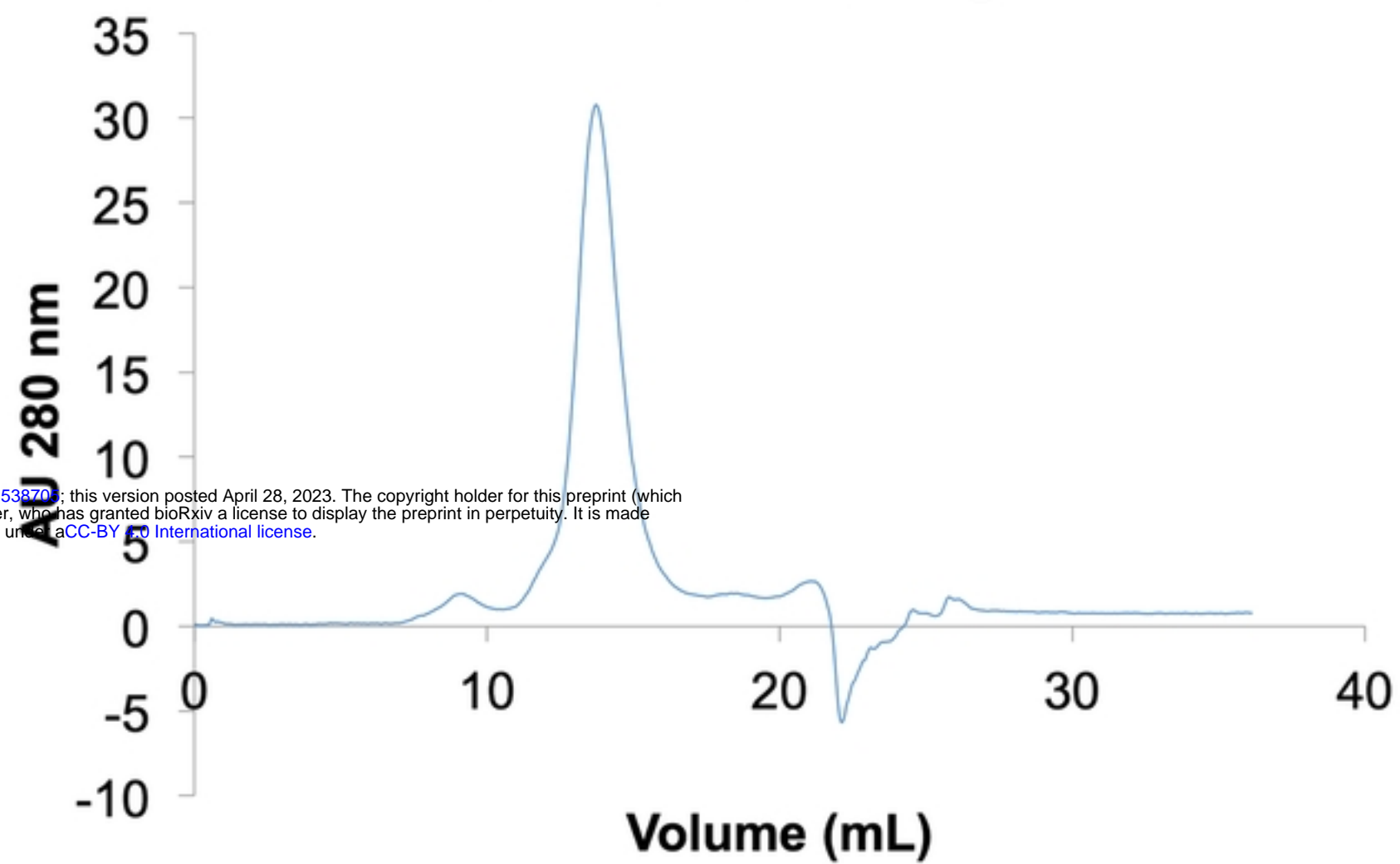


Figure 6

A.**B.**

Gel Filtration Chromatogram



bioRxiv preprint doi: <https://doi.org/10.1101/2023.04.28.538709>; this version posted April 28, 2023. The copyright holder for this preprint (which was not certified by peer review) is the author/funder, who has granted bioRxiv a license to display the preprint in perpetuity. It is made available under aCC-BY 4.0 International license.

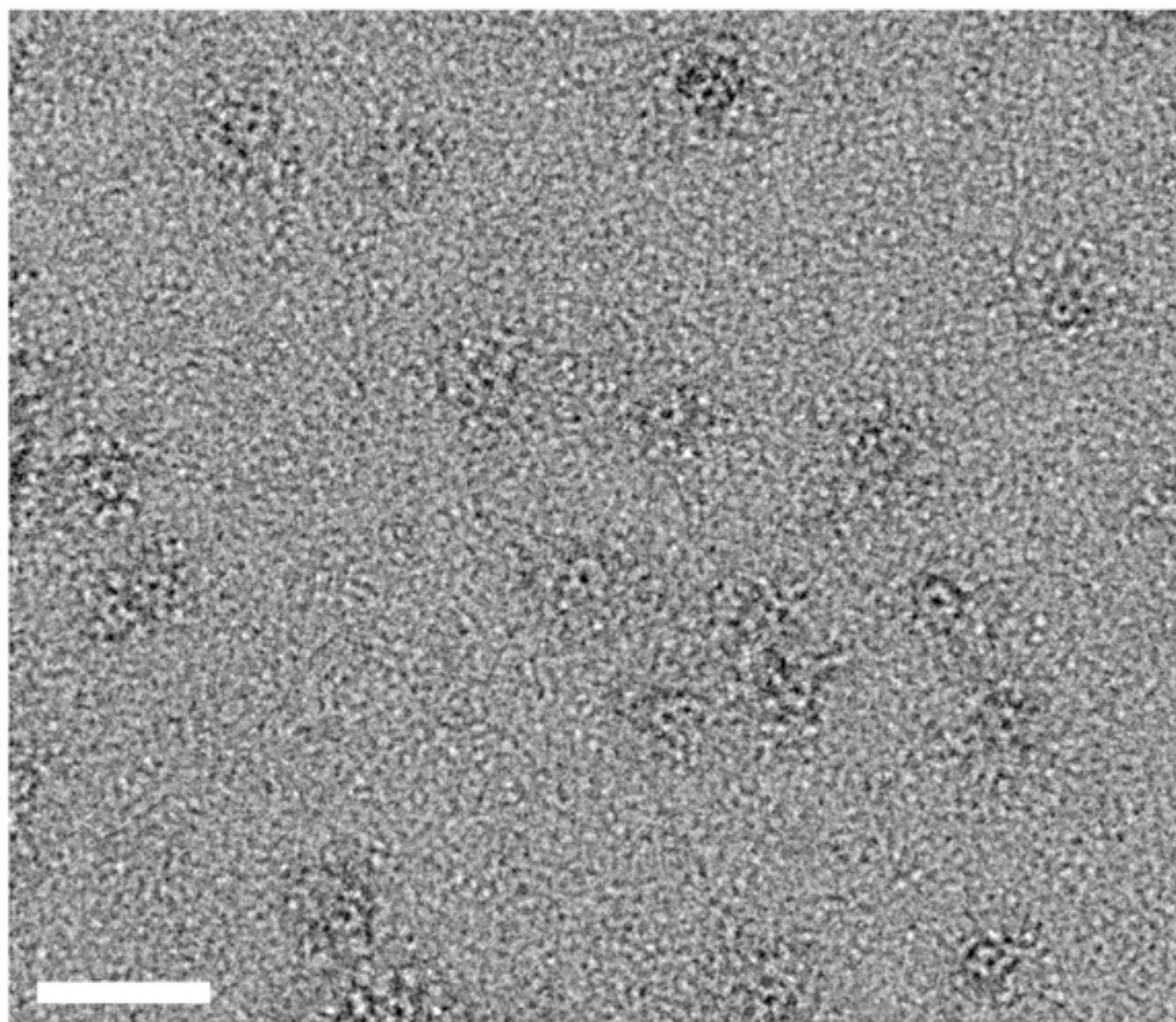
C.

Figure 7